Analytical formulas for Coulomb integrals involved in scattering problems

L. U. Ancarani
Department of Applied Mathematics and Theoretical Physics, University of Cambridge, Silver Street, Cambridge CB3 9EW, United Kingdom

P. A. Hervieux
Laboratoire de Physique Moléculaire et des Collisions, Institut de Physique, Technopôle 2000, 57078 Metz, France

(Received 22 December 1997)

Radial matrix elements of multipole type involving the product of two Coulomb functions appear in many problems of theoretical atomic physics. Here we investigate some of their properties, with a generalization which includes the possibility of having the two functions related to two different charges. These would typically appear in calculations of ionization cross sections, going beyond the well studied case where the two charges are equal (elastic scattering or discrete excitation). We provide analytical formulas for the evaluation of matrix elements and recursion relations connecting them, both in the exact quantal formulation and in the WKB approximation. These theoretical results are illustrated by considering, within the Coulomb projected Born model, the electron impact ionization of Mg^+ and Ar^{7+} with a relatively moderate incident energy. The radial matrix elements are evaluated with our exact quantal formulas and in the WKB approximation. The agreement is impressive, and is reflected in the values of triple, double, and single differential cross sections. Finally, a further study shows how the semiclassical approximation yields a very good estimate of single cross sections. [S1050-2947(98)05407-9]

PACS number(s): 34.80.Kw, 34.80.Dp

I. INTRODUCTION

In many problems of atomic physics, integrals involving the product of two Coulomb functions appear in the theoretical partial wave formulations. Indeed, in model calculations of scattering amplitudes where Coulomb wave functions $\mathcal{F}_{\mathbf{k}}^{\pm}(\mathbf{r})$ are involved, one conveniently separates the angular from the radial part, with the well known partial wave expansion

$$\mathcal{F}_{\mathbf{k}}^{\pm}(\mathbf{r})=\sum_{l,m} 4\pi(i)^l e^{\pm i\delta_l}\frac{1}{kr}F_l(k,z;r)Y_{l,m}^*(\hat{k})Y_{l,m}(\hat{r}), \tag{1}$$

where $Y_{l,m}$ are spherical harmonics, $\delta_l=\arg\Gamma(l+1+i\eta)$ are the Coulomb phase shifts, and $F_l(k,z;r)$ are the Coulomb radial wave functions for given charge z and momentum k ($\eta=z/k$ is the Sommerfeld parameter),

$$F_l(k,z;r)=\frac{|\Gamma(l+1+i\eta)|}{2\Gamma(2l+2)}e^{-\eta\pi/2}(2kr)^{l+1}e^{-ikr} \times {}_1F_1(l+1-i\eta,2l+2,2ikr). \tag{2}$$

One has then to evaluate radial Coulomb integrals of multipole type and we shall investigate here some of their properties restricting ourselves to the nonrelativistic case. In the notation of Alder *et al.* [1] the Coulomb integrals in question, often called matrix elements, are written as follows:

$$\mathcal{M}_{l_i,l_f}^{-\lambda-1}=\frac{1}{k_ik_f}\int_0^\infty F_{l_i}(k_i,z_i;r)\frac{1}{r^{\lambda+1}}F_{l_f}(k_f,z_f;r)dr, \tag{3}$$

where z_i and z_f are not necessarily equal, and can be either positive or negative corresponding to a repulsive or an attractive Coulomb potential depending on the charge of the projectile. The case z_i or z_f equal to zero corresponds to zero potential, for which the Coulomb partial wave functions reduce to Bessel functions. $\lambda\geqslant 0$ describes the multipole considered, while l_i and l_f are the angular momenta for the initial and final states of a collision process. The conservation of angular momentum implies that only the cases for which $l_i-l_f=-\lambda,-\lambda+2,\ldots,\lambda$ are of physical interest.

For electron impact collision processes where the initial and final charges z_i and z_f are equal (elastic scattering or discrete excitation), formulas for such integrals have been derived and extensively studied in the past: Alder *et al.* [1] in the frame of Coulomb excitations of nuclei while Burgess *et al.* [2,3] similarly for atomic targets. For certain ranges of Sommerfeld parameters, the accurate numerical computation of such integrals is not an easy task due to the highly oscillatory nature of the integrand; various formulas, tables, and details of numerical techniques can be found in the appendix of [2]. High precision in the evaluation of Coulomb integrals is often required in collision calculations since cancellations may occur in the partial wave summations. Also, in some cases (typically for a dipole excitation of positive ions), a large number of matrix elements (3) are needed for converged calculations of scattering amplitudes: recursion relations are then a powerful tool to cope with this issue [1,4].

In the first part of this contribution, we extend a series of properties for matrix elements (3) to the general case, including the possibility $z_i\neq z_f$. The corresponding integrals would appear, for example, in partial wave calculations of scattering amplitudes for ionization processes where the initial and final target charges differ. Along the lines of [1], we provide formulas for evaluating the matrix elements (3), and a series

of useful recursion relations linking matrix elements of similar or different multipolarity. The results provided here can be seen as a generalization of some of those given, for $z_i = z_f$, in [1]. We then investigate the matrix elements (3) in the WKB approximation [1] which, under certain appropriate conditions, has proved to be a very useful approach in many aspects of scattering problems [5–8]. The effectiveness of the WKB method was illustrated in a preceding publication by Hervieux and Guet [9] on the study of excitation ($z_i = z_f$) of alkali-metal-like ions by electron impact. In the WKB approximation the matrix elements are expressed in terms of an integral which is directly related to the semiclassical picture. Here, we extend this integral expression (given, for example, in [1]) to the general case, including $z_i \neq z_f$. For the monopole case, one can express the matrix element in terms of Hankel functions. For higher multipoles, we are able to derive analytical formulas which link matrix elements of different multipolarities. The classical limit of the quantal result is also briefly discussed. As an illustration of our general formulas we present a selection of numerical results for the monopole, dipole, and quadrupole matrix elements (often dominant in scattering problems) for two scattering situations: the electron impact excitation ($z_i = z_f = -Z$) and ionization ($z_i = -Z$, $z_f = -Z-1$) of positively charged targets (Mg^+, $Z=1$ and Ar^{7+}, $Z=7$). These allow us to verify the numerical validity of some of our recursion relations, and to make a comparison of the quantal and WKB results showing the surprisingly good quality of the latter.

In the second part, we would like to demonstrate the usefulness of our theoretical formulation with a simple study of a practical case, the ionization of a positive ion by electron impact. We first provide the quantal formulas, in the Coulomb projected Born (CPB) approximation [10], for the singly, doubly, and triply differential cross sections (denoted, respectively, SDCS, DDCS, and TDCS) showing how the matrix elements (3) with $z_i \neq z_f$ appear. Since there is a close link with the WKB approximation to the matrix elements, we then consider the semiclassical (SC) approximation [1,5] and provide formulas for singly and doubly differential cross sections. In recent years, the SC approximation has been ''rediscovered'' in various domains: electron elastic scattering by atoms [6], discrete excitation of positive ions [9], inner-shell ionization by heavy particles [7]. Finally, we show the numerical results obtained for the electron impact ionization of the valence electron of the alkali-metal-like ions Mg^+ and Ar^{7+} in their ground state. A comparison between the quantal results, and their WKB and semiclassical counterparts is presented. We would like to make clear the fact that we have no intention, with the CPB approximation, of producing accurate ionization cross sections. The example is taken as a means of illustrating how the analytical results we provide in the first part of this contribution may be useful when solving scattering problems.

II. THEORY: ANALYTICAL FORMULAS FOR RADIAL COULOMB INTEGRALS

A. Exact Coulomb functions

We start by looking at how the formulas to evaluate matrix elements (3) provided in [1] need to be modified to include the case $z_i \neq z_f$, and then tackle the issue of recursion relations. Two Sommerfeld parameters are involved, $\eta_i = z_i/k_i$ and $\eta_f = z_f/k_f$; for convenience we define $\xi = \eta_f - \eta_i$.

(a) $\lambda = 0$. Equation (II.B.56) of [1] is modified as follows:

$$\mathcal{M}_{l,l}^{-1} = e^{-(\pi/2)\xi}(k_i - k_f)^{-2}\left(\frac{k_i - k_f}{k_i + k_f}\right)^{i(\eta_i+\eta_f)}\left(\frac{4k_ik_f}{(k_i-k_f)^2}\right)^{l} \times \frac{|\Gamma(l+1+i\eta_i)||\Gamma(l+1+i\eta_f)|}{\Gamma(2l+2)} \times F\left(l+1-i\eta_i, l+1-i\eta_f, 2l+2; \frac{-4k_ik_f}{(k_i-k_f)^2}\right) \quad (4)$$

and relation (II.B.59) of [1] still holds,

$$\mathcal{M}_{l,l}^{-1}(k_i,\eta_i;k_f,\eta_f) = e^{-\pi\xi}\mathcal{M}_{l,l}^{-1}(k_i,-\eta_i;k_f,-\eta_f). \quad (5)$$

(b) $\lambda \geq 1$. For multipoles $\lambda \geq 1$, expression (II.B.58) of [1] for $\mathcal{M}_{l+\lambda,l}^{-\lambda-1}$ is changed into

$$\mathcal{M}_{l+\lambda,l}^{-\lambda-1} = e^{(\pi/2)\xi}(2k_i)^{\lambda-2}\left(\frac{k_f}{k_i}\right)^{l}\frac{|\Gamma(l+1+i\eta_f)|}{|\Gamma(l+1+\lambda+i\eta_i)|} \times \left\{\frac{|\Gamma(\lambda+i\xi)|^2}{\Gamma(2\lambda)}F_2\left(-2\lambda+1, l+1-i\eta_f, l+1+i\eta_f, -\lambda+1-i\xi, -\lambda+1+i\xi; \frac{k_i-k_f}{2k_i}, \frac{k_i-k_f}{2k_i}\right)\right. + 2\mathcal{R}e\left[\left(\frac{k_f-k_i}{2k_i}\right)^{\lambda+i\xi}\frac{\Gamma(l+1+\lambda-i\eta_i)\Gamma(-\lambda-i\xi)}{\Gamma(l+1-i\eta_f)} \times F_2\left(-\lambda+1+i\xi, l+1+\lambda-i\eta_i, l+1+i\eta_f, \lambda+1+i\xi, -\lambda+1+i\xi; \frac{k_i-k_f}{2k_i}, \frac{k_i-k_f}{2k_i}\right)\right]\Bigg\}, \quad (6)$$

where F_2 is a generalized hypergeometric function, one of the so-called Appell functions. In Eq. (6), the first function F_2 reduces to a polynomial since its first parameter is a negative integer. In particular, for the dipole and quadrupole cases one finds

$$F_2(-2\lambda+1,\ldots)=\begin{cases}\dfrac{\eta_i}{z_i\xi}(z_f-z_i) & (\lambda=1)\\ \dfrac{\eta_i}{2}\dfrac{A}{\eta_f^2 z_i^3\xi(1+\xi^2)} & (\lambda=2),\end{cases} \tag{7}$$

where

$$\begin{aligned}A=&z_i z_f^2\xi(\eta_i+\eta_f)+(z_f-z_i)\\ &\times[2\eta_i^2\eta_f^2(z_f-z_i)^2-\eta_f^2 z_i z_f\\ &-(3l+4)\eta_i^2 z_f^2+(3l+5)\eta_f^2 z_i^2],\end{aligned}$$

which is an extension of Eq. (II.B.60) of [1]. As indicated in [1], the second function F_2 in expression (6) can be reduced to a single function F_1 by use of

$$\begin{aligned}F_2(\alpha,\beta,\beta',\gamma,\alpha;x,y)=&(1-y)^{-\beta'}\\ &\times F_1\left(\beta,\alpha-\beta',\beta',\gamma;x,\frac{x}{1-y}\right),\end{aligned} \tag{8}$$

where the function F_1 can then be computed using the series

$$F_1(\alpha,\beta,\beta',\gamma;x,y)=\sum_{m,n}\frac{\alpha_{m+n}\beta_m\beta'_n}{\gamma_{m+n}m!n!}x^m y^n, \qquad |x|<1,\quad |y|<1 \tag{9}$$

where $\alpha_n=\Gamma(\alpha+n)/\Gamma(\alpha)$.

In the case of vanishing energy loss ($k_i=k_f=k$), expression (6) for $\mathcal{M}^{-\lambda-1}_{l+\lambda,l}$ ($\lambda\geqslant 1$) is especially simple,

$$\mathcal{M}^{-\lambda-1}_{l+\lambda,l}=e^{(\pi/2)\xi}(2k)^{\lambda-2}\left|\frac{\Gamma(l+1+i\eta_f)}{\Gamma(l+1+\lambda+i\eta_i)}\right|\frac{|\Gamma(\lambda+i\xi)|^2}{\Gamma(2\lambda)}, \tag{10}$$

which is an extension of Eq. (II.E.74) [1], the latter being valid only for the case $z_i=z_f$. This result can be of use, for example, in (e-3e) calculations; indeed, in the so-called two step process (TS1) [11] use is made of the second Born approximation, and in the partial wave expansion of the corresponding matrix elements, the situation $k_i=k_f$ and $z_i\neq z_f$ appears.

The matrix elements $\mathcal{M}^{-\lambda-1}_{l,l+\lambda}$ can be directly obtained from $\mathcal{M}^{-\lambda-1}_{l+\lambda,l}$ through the simple relation

$$\mathcal{M}^{-\lambda-1}_{l,l+\lambda}(k_i,\eta_i;k_f,\eta_f)=\mathcal{M}^{-\lambda-1}_{l+\lambda,l}(k_f,\eta_f;k_i,\eta_i). \tag{11}$$

Moreover, the matrix elements corresponding to the repulsive and attractive Coulomb fields are related, for any value of λ, through the relation

$$\mathcal{M}^{-\lambda-1}_{l,l+\lambda}(k_i,\eta_i;k_f,\eta_f)=e^{-\pi\xi}\mathcal{M}^{-\lambda-1}_{l,l+\lambda}(k_i,-\eta_i;k_f,-\eta_f), \tag{12}$$

however, generally, for $\lambda>1$

$$\mathcal{M}^{-\lambda-1}_{l+\lambda,l}(k_i,\eta_i;k_f,\eta_f)\neq e^{-\pi\xi}\mathcal{M}^{-\lambda-1}_{l+\lambda,l}(k_i,-\eta_i;k_f,-\eta_f). \tag{13}$$

In the case $z_i=z_f$, and only for $\lambda=1$, one has the equality

$$\mathcal{M}^{-2}_{l+1,l}(k_i,\eta_i;k_f,\eta_f)=e^{-\pi\xi}\mathcal{M}^{-2}_{l+1,l}(k_i,-\eta_i;k_f,-\eta_f). \tag{14}$$

So far, we have been dealing with matrix elements for which the angular momentum selection rule is satisfied. We will now show how the matrix elements given above, and others with different combinations of multipolarity and angular momenta, may be efficiently related via recursion relations. Generally speaking, the latter constitute a powerful tool for the evaluation of large numbers of matrix elements, thus avoiding to have to evaluate hypergeometric functions [see Eqs. (4) and (6)] for each angular momentum value. Moreover, for large angular momenta and certain ranges of Sommerfeld parameters, it is numerically hard to reach proper convergence in calculating series (9), and analytical relations between matrix elements allow one to overcome the difficulty. Recursion relations also provide us with a way of evaluating matrix elements with broken selection rule.

For $z_i=z_f$ recursion relations between matrix elements are given in [1,4], and we now extend some of them so that they are valid also for the case $z_i\neq z_f$. We start from relations (14.2.1) and (14.2.2) of [12] satisfied by the Coulomb wave functions and consider matrix elements (3) with λ replaced by $\lambda+1$. By partial integration one obtains, for $l_i+l_f+1-\lambda>0$, general formulas connecting matrix elements of multipolarity differing by one,

$$\begin{aligned}(\lambda+l_i-l_f)\mathcal{M}^{-\lambda-2}_{l_i,l_f}=&\frac{\alpha^i_{l_i-1}}{l_i}\mathcal{M}^{-\lambda-1}_{l_i-1,l_f}-\frac{\alpha^f_{l_f}}{l_f+1}\mathcal{M}^{-\lambda-1}_{l_i,l_f+1}\\ &+\left(\frac{z_f}{l_f+1}-\frac{z_i}{l_i}\right)\mathcal{M}^{-\lambda-1}_{l_i,l_f},\end{aligned} \tag{15}$$

$$\begin{aligned}(\lambda+l_f-l_i)\mathcal{M}^{-\lambda-2}_{l_i,l_f}=&\frac{\alpha^f_{l_f-1}}{l_f}\mathcal{M}^{-\lambda-1}_{l_i,l_f-1}-\frac{\alpha^i_{l_i}}{l_i+1}\mathcal{M}^{-\lambda-1}_{l_i+1,l_f}\\ &+\left(\frac{z_i}{l_i+1}-\frac{z_f}{l_f}\right)\mathcal{M}^{-\lambda-1}_{l_i,l_f},\end{aligned}$$

where we have introduced

$$\alpha^a_l=[k_a^2(l+1)^2+z_a^2]^{1/2},$$

the superscript a indicating that the momentum k_a and charge z_a are involved. It is quite easy to see how this result reduces to a known formula in the case $z_i=z_f$; indeed, taking $l_i=l_f+1=l+1$ in the first or $l_f=l_i+1=l+1$ in the second, the last term drops out and one recovers formula (II.B.68) of [1]. One may also derive another formula, similar to Eq. (15),

$$(\lambda+l_i+l_f+1)\mathcal{M}^{-\lambda-2}_{l_i,l_f}=\frac{\alpha^i_{l_i-1}}{l_i}\mathcal{M}^{-\lambda-1}_{l_i-1,l_f}+\frac{\alpha^f_{l_f-1}}{l_f}\mathcal{M}^{-\lambda-1}_{l_i,l_f-1}-\left(\frac{z_i}{l_i}+\frac{z_f}{l_f}\right)\mathcal{M}^{-\lambda-1}_{l_i,l_f} \tag{16}$$

and, from these, another one valid for $\lambda\neq l_f-l_i$,

$$(2l_f+1)\left(\frac{z_i}{l_i}-\frac{z_f(\lambda+l_i)}{l_f(l_f+1)}\right)\mathcal{M}^{-\lambda-1}_{l_i,l_f}=\frac{\alpha^i_{l_i-1}}{l_i}(2l_f+1)\mathcal{M}^{-\lambda-1}_{l_i-1,l_f}-(\lambda+l_i+l_f+1)\frac{\alpha^f_{l_f}}{l_f+1}\mathcal{M}^{-\lambda-1}_{l_i,l_f+1}-(\lambda+l_i-l_f)\frac{\alpha^f_{l_f-1}}{l_f}\mathcal{M}^{-\lambda-1}_{l_i,l_f-1}, \tag{17}$$

which links matrix elements of same multipolarity. To demonstrate explicitly the information contained in these relations, we now consider the first two multipoles.

(a) $\lambda=0$. By taking $l_i=l_f+1=l+1$ and $l_f=l_i+1=l+1$ in the two relations (15) one obtains

$$(z_i-z_f)\mathcal{M}^{-1}_{l+1,l}=\alpha^i_l\mathcal{M}^{-1}_{l,l}-\alpha^f_l\mathcal{M}^{-1}_{l+1,l+1}-(l+1)\mathcal{M}^{-2}_{l+1,l}, \tag{18}$$

$$(z_i-z_f)\mathcal{M}^{-1}_{l,l+1}=-\alpha^f_l\mathcal{M}^{-1}_{l,l}+\alpha^i_l\mathcal{M}^{-1}_{l+1,l+1}+(l+1)\mathcal{M}^{-2}_{l,l+1}.$$

We notice here that the left-hand sides feature matrix elements with broken selection rule for angular momentum. These types of matrix elements appear only in the context $z_i\neq z_f$ (see prefactor) and are related to the fact that the first F_2 is not zero for $\lambda=1$ [see Eq. (7)]. They are given in terms of matrix elements whose evaluation is prescribed above [formulas (4) and (6)]. Only one matrix element of each kind needs to be evaluated as one can derive, from Eq. (15) with $l_i=l_f=l$, the following recursion relations:

$$(l+1)\alpha^i_{l-1}\mathcal{M}^{-1}_{l-1,l}-l\alpha^f_l\mathcal{M}^{-1}_{l,l+1}=[(l+1)z_i-lz_f]\mathcal{M}^{-1}_{l,l}, \tag{19}$$

$$(l+1)\alpha^f_{l-1}\mathcal{M}^{-1}_{l,l-1}-l\alpha^i_l\mathcal{M}^{-1}_{l+1,l}=[(l+1)z_f-lz_i]\mathcal{M}^{-1}_{l,l}.$$

Similarly, using Eq. (16) instead, one obtains an expression for another matrix element, $\mathcal{M}^{-2}_{l,l}$, with broken selection rule

$$l(2l+1)\mathcal{M}^{-2}_{l,l}=\alpha^i_{l-1}\mathcal{M}^{-1}_{l-1,l}+\alpha^f_{l-1}\mathcal{M}^{-1}_{l,l-1}-(z_i+z_f)\mathcal{M}^{-1}_{l,l}. \tag{20}$$

From the results above, one may derive the following interesting relations:

$$\alpha^i_l\mathcal{M}^{-2}_{l+1,l}-\alpha^f_{l-1}\mathcal{M}^{-2}_{l,l-1}=\alpha^i_{l-1}\mathcal{M}^{-2}_{l-1,l}-\alpha^f_l\mathcal{M}^{-2}_{l,l+1}=\frac{1}{2}(k_i^2-k_f^2)\mathcal{M}^{-1}_{l,l}, \tag{21}$$

$$\frac{2\alpha^i_l\alpha^f_l}{l+1}\mathcal{M}^{-1}_{l+1,l+1}-(2l+1)\left(k_i^2+k_f^2+\frac{2z_iz_f}{l(l+1)}\right)\mathcal{M}^{-1}_{l,l}+\frac{2\alpha^i_{l-1}\alpha^f_{l-1}}{l}\mathcal{M}^{-1}_{l-1,l-1}=0. \tag{22}$$

The latter can be seen as an extension of formula (II.B.66) of [1] as it reduces to it for $z_i=z_f$. Moreover, a recursion relation linking the same matrix elements as in Eq. (II.B.70) of [1] can be written but will feature on the right-hand side a term proportional to $(z_i-z_f)\mathcal{M}^{-1}_{l,l-1}$. For practical purposes, relation (21) provides a much easier alternative.

(b) $\lambda=1$. For $l_i=l_f=l>0$, relation (15) gives

$$l(l+1)\mathcal{M}^{-3}_{l,l}=(l+1)\alpha^i_{l-1}\mathcal{M}^{-2}_{l-1,l}-l\alpha^f_l\mathcal{M}^{-2}_{l,l+1}-[(l+1)z_i-lz_f]\mathcal{M}^{-2}_{l,l}. \tag{23}$$

The last term can be replaced by the result obtained from Eq. (17),

$$(2l+1)(z_i-z_f)\mathcal{M}^{-2}_{l,l}=\alpha^i_{l-1}(2l+1)\mathcal{M}^{-2}_{l-1,l}-2l\alpha^f_l\mathcal{M}^{-2}_{l,l+1}-\alpha^f_{l-1}\mathcal{M}^{-2}_{l,l-1} \tag{24}$$

yielding, for $z_i\neq z_f$,

$$(2l+1)l(l+1)(z_f-z_i)\mathcal{M}^{-3}_{l,l}=\alpha^i_{l-1}(2l+1)z_f\mathcal{M}^{-2}_{l-1,l}-l\alpha^f_l(z_i+z_f)\mathcal{M}^{-2}_{l,l+1}-\alpha^f_{l-1}[(l+1)z_i-lz_f]\mathcal{M}^{-2}_{l,l-1}. \tag{25}$$

For $\mathcal{M}^{-3}_{l+1,l}$, we take $l_i=l_f+1=l+1$ in Eq. (15) to obtain

$$2(l+1)\mathcal{M}^{-3}_{l+1,l}=(z_f-z_i)\mathcal{M}^{-2}_{l+1,l}+\alpha^i_l\mathcal{M}^{-2}_{l,l}-\alpha^f_l\mathcal{M}^{-2}_{l+1,l+1}, \tag{26}$$

where the last two terms can be replaced using Eq. (24).

We have therefore shown how one can evaluate matrix elements not covered by formulas (4) and (6), including those with selection rule for angular momentum which is broken (e.g., $\mathcal{M}^{-1}_{l+1,l}$, $\mathcal{M}^{-2}_{l,l}$, $\mathcal{M}^{-3}_{l+1,l}$) and unbroken ($\mathcal{M}^{-3}_{l,l}$). Alternative combinations of expressions given above would yield other relations, but we do not wish here to cover them all. It is obvious that one can proceed similarly for higher values of λ. Suppose one wishes to compute all the matrix elements satisfying the selection rule for $\lambda=3$: $\mathcal{M}^{-4}_{l+3,l}$ can be evaluated through Eq. (6), $\mathcal{M}^{-4}_{l+1,l}$ through relation (15) in terms of $\mathcal{M}^{-3}_{l,l}$, $\mathcal{M}^{-3}_{l+1,l+1}$, and $\mathcal{M}^{-3}_{l+1,l}$ [$\mathcal{M}^{-4}_{l,l+3}$ and $\mathcal{M}^{-4}_{l,l+1}$ are directly given by relation (11)].

Finally, before closing this subsection, we would like to mention that it can sometimes be useful to express radial integrals of type (3) of a given multipolarity λ in terms of others with $\lambda+1$. In the context of the Coulomb Born approximation for the calculation of excitation cross sections, Nakazaki [13] has derived such links, based on the property (13.4.10) [12] of the confluent hypergeometric function. These can be easily generalized to include the case $z_i\neq z_f$.

B. WKB approximation

Under certain conditions, the WKB approximation provides a good approach in many scattering problems [1,5–8]. In a preceding publication [9], the WKB approximation was employed and shown to be effective for the study of excitation ($z_i=z_f$) of alkali-metal-like ions by electron impact.

The generalization, including the possibility $z_i \neq z_f$, of the WKB formula for the matrix elements reads

$$\mathcal{M}^{-\lambda-1}_{l_i,l_i+\mu} = \frac{\tilde{k}^{\lambda-2}}{4\tilde{\eta}^{\lambda}} \mathcal{I}^{\lambda\mu}(\epsilon,\xi',\alpha), \tag{27}$$

$$\mathcal{I}^{\lambda\mu}(\epsilon,\xi',\alpha) = \int_{-\infty}^{+\infty} e^{i\xi'[\epsilon\sinh(x)+x+(\alpha/\xi')x]} \times \frac{[\cosh(x)+\epsilon+i\sqrt{\epsilon^2-1}\sinh(x)]^{\mu}}{[\epsilon\cosh(x)+1]^{\lambda+\mu}} dx, \tag{28}$$

where the different quantities are defined as

$$\mu = l_i - l_f, \quad \tilde{l} = \frac{l_i+l_f}{2},$$

$$\tilde{k} = \sqrt{k_i k_f}, \quad \tilde{z} = \mathrm{sgn}(z_i)\sqrt{z_i z_f}, \quad \tilde{\eta} = \frac{\tilde{z}}{\tilde{k}},$$

$$\epsilon = \frac{[\tilde{\eta}^2 + (\tilde{l}+\frac{1}{2})^2]^{1/2}}{\tilde{\eta}},$$

$$\alpha = -(z_i - z_f)/\tilde{k}, \quad \xi' = (k_i - k_f)\frac{\tilde{\eta}}{\tilde{k}}.$$

Clearly, for $z_i = z_f$, ξ' reduces to ξ and Eq. (27) to expression (II.B.100) of [1]. Note that here we have chosen the geometric mean for $\tilde{\eta}$ and $\tilde{k}$; indeed, we have observed that numerical results obtained with this choice (see subsections II E and III C) are slightly better than those obtained with arithmetic means. The latter, however, must be used when one of the two charges is zero, i.e., for the case of ionization of a singly charged negative ion or of a neutral atom. As indicated in Sec. II.E.4 of [1], the numerical calculation of Eq. (28) is greatly facilitated if one translates the integration path by an amount of $i\pi/2$, as this decreases the oscillating behavior of the integrand.

For $\lambda = 0$ the matrix element (27) can be expressed as

$$\mathcal{M}^{-1}_{l,l} = \frac{1}{4\tilde{k}^2}\mathcal{I}^{00}(\epsilon,\xi',\alpha),$$

$$\mathcal{I}^{00}(\epsilon,\xi',\alpha) = 2e^{-(\pi/2)(\xi'+\alpha)} K_{i(\xi'+\alpha)}(\xi'\epsilon), \tag{29}$$

where $K_\nu(z)$ denotes the Hankel function defined by

$$K_\nu(z) = \int_0^\infty e^{-z\cosh(t)+\nu t} dt. \tag{30}$$

Although relation (29) provides an effective way of evaluating the monopole matrix element in the WKB approximation, one has to keep in mind that such terms would not appear in atomic collision calculations [see, for example, Eq. (43) below]. For this very same reason, and for the fact that in nuclear excitation the distance of closest approach is far larger than the nuclear size itself, Alder *et al.* [1] have not provided in Sec. II.E.5, for $\lambda = 0$, an analytical result like Eq. (29).

For $\lambda = 1$, on the other hand, they give a formula (II.E.57), which expresses the matrix element in terms of a Hankel function and its first derivative. An equivalent expression, for $z_i \neq z_f$, was not found because of the extra exponential term in Eq. (28). However, we were able to find the following formulas connecting WKB matrix elements of different λ and μ:

$$\epsilon\mathcal{I}^{1\pm1} = \mp\xi'\sqrt{\epsilon^2-1}\mathcal{I}^{00} + (1 \mp \alpha\sqrt{\epsilon^2-1})\mathcal{I}^{10} + (\epsilon^2-1)\mathcal{I}^{20} \tag{31}$$

$$= \mp\frac{1}{\sqrt{\epsilon^2-1}}\left[[\xi'(\epsilon^2-1)-\alpha]\mathcal{I}^{00} \pm \epsilon\xi'\sqrt{\epsilon^2-1}\frac{d\mathcal{I}^{00}}{d\epsilon} + \alpha\epsilon\mathcal{I}^{0\pm1} \right], \tag{32}$$

where we have omitted the arguments of $\mathcal{I}^{\lambda\mu}(\epsilon,\xi',\alpha)$ for the sake of compactness. One can appreciate here the similarity of Eq. (32) with our quantal result (18), i.e., the appearance of a matrix element with broken selection rule of angular momentum; for $z_i = z_f$, this contribution disappears, and Eq. (32) reduces to the above-mentioned Eq. (II.E.57) of [1]. Result (31) is given here because of its numerical usefulness; indeed, compared to the elements $\mathcal{I}^{\lambda\mu}$, those with $\mu = 0$ have an integrand which decreases faster for large values of the integration variable, and are therefore easier to calculate.

In the case $z_i = z_f$, Alder and Winther [14] provided several formulas connecting matrix elements of different λ and μ [incidentally, we would like to point out two typographical mistakes in that paper: (a) the second 4 of the $\lambda = 3$ result in Eq. (13) should be 2; (b) the 3 of the second line of Eq. (17) should be 1]. These were easily generalized to include the possibility $z_i \neq z_f$, and more were derived. Here we give only the generalization of their formula (15), valid for $\lambda > 0$,

$$\epsilon\frac{d\mathcal{I}^{\lambda0}}{d\epsilon} = -(\lambda+1)\epsilon\mathcal{I}^{\lambda+11} - \xi'\sqrt{\epsilon^2-1}\mathcal{I}^{\lambda0} + \frac{\alpha}{\lambda}[\xi'\mathcal{I}^{\lambda-10} + \alpha\mathcal{I}^{\lambda0} - \lambda\sqrt{\epsilon^2-1}\mathcal{I}^{\lambda+10}], \tag{33}$$

which, for numerical purposes, can be more conveniently written

$$\epsilon\frac{d\mathcal{I}^{\lambda0}}{d\epsilon} = -(\lambda+1)[\mathcal{I}^{\lambda+10} + (\epsilon^2-1)\mathcal{I}^{\lambda+20}] + \frac{\alpha}{\lambda}[\xi'\mathcal{I}^{\lambda-10} + \alpha\mathcal{I}^{\lambda0}]. \tag{34}$$

C. Classical limit

We consider now the so-called classical limit, that is, for $|l_i - i\eta_i| \gg 1$, $|l_f - i\eta_f| \gg 1$ and ξ finite (see Sec. II.E.4 in [1]). In this limit the quantal result (6) for $\lambda \geqslant 1$ is transformed, through a confluence, into

$$\mathcal{M}^{-\lambda-1}_{l+\lambda,l}=\frac{\tilde{k}^{\lambda-2}}{4\tilde{\eta}^{\lambda}}2^{\lambda}\sin^{\lambda}\frac{\theta}{2}e^{-\xi(\theta/2-\pi/2)}e^{-\xi'\cot\theta/2}$$
$$\times\left\{\frac{|\Gamma(\lambda+i\xi)|^2}{\Gamma(2\lambda)}\Psi_2(-2\lambda+1,-\lambda+1-i\xi,-\lambda+1+i\xi;z',z'^{*})\right.$$
$$\left.+2\mathrm{Re}\{(-)^{\lambda}e^{-\pi\xi}z'^{\lambda+i\xi}\Gamma(-\lambda-i\xi)\Psi_2(-\lambda+1+i\xi,\lambda+1+i\xi,-\lambda+1+i\xi;z',z'^{*})\}\right\}, \quad (35)$$

with $\theta=2\arcsin(1/\epsilon)$ and $z'=(\xi'/2)(\cot\theta/2-i)$, and where

$$\Psi_2(\alpha,\gamma,\gamma';x,y)=\sum_{m,n}\frac{\alpha_{m+n}}{\gamma_m\gamma'_n m!n!}x^m y^n \quad (36)$$

is a confluent Appell function which is convergent for all x and y. Together with relation (27), our result (35) constitutes an extension of formula (II.E.50) of [1] [in that formula $(-)^{\lambda}$ is missing in front of the second Ψ_2]. One can mathematically show that the classical limit of Eq. (6) yields the WKB formulas (27) and (28) (see [4] for the $z_i=z_f$ case). We have verified that this is indeed the case in our numerical investigation (see subsection II E): the agreement is perfect for $z_i=z_f$, almost perfect for $z_i\neq z_f$, and better for larger $|z_i|$.

Another interesting limit is the one of large orbital angular momenta, $\tilde{l}\gg 1$ (see Sec. II.E.7 of [1]). The classical limit result (35) given above still holds, irrespective of the value of $\tilde{\eta}$. However, if $\tilde{l}\gg|\tilde{\eta}|$ the deflection angle θ of the associated classical orbit is small ($\theta\sim 2\tilde{\eta}/\tilde{l}$) and the orbits approach straight lines (see also subsection III B). Then $\epsilon\gg 1$, and we may neglect $e^{i(\xi'+\alpha)x}$ in Eq. (28); with arguments similar to those given in Sec. II.E.7 of [1], we find ($\lambda\geqslant 1$)

$$\mathcal{M}^{-\lambda-1}_{l+\lambda,l}\simeq\frac{\tilde{k}^{\lambda-2}}{4\tilde{\eta}^{\lambda}}\frac{2\pi}{\Gamma((\lambda-\mu+1)/2)}e^{-(\pi/2)(\xi'+\alpha)}e^{-\xi'\tilde{l}/\tilde{\eta}}$$
$$\times\xi'^{(\lambda-\mu-1)/2}\left(\frac{2\tilde{l}}{\tilde{\eta}}\right)^{-(\lambda+\mu+1)/2}. \quad (37)$$

D. Other considerations

In calculations for elastic scattering or discrete excitation of neutral targets where matrix elements (3) would appear, we have $z_i=z_f=0$ and the integrand reduces to a product of Bessel functions times a power of r. Since the charge is equal, such integrals fall into the category studied in [1]; in particular, they can be written in terms of an ordinary hypergeometric function [see Eq. (II.E.31) in [1]]. The cases of ionization by an electron (positron) of a neutral target ($z_i=0, z_f=\mp 1$) or of a singly charged negative ion ($z_i=\pm 1, z_f=0$) are interesting since the radial integrals contain both a Bessel and a Coulomb function. The properties outlined in Sec. II A may be used.

For the evaluation of integrals (3), one may adopt a different approach, by splitting the integration into two parts: the first, which runs from $r=0$ to a certain R, can be performed with standard numerical quadrature; in the second, from $r=R$ to infinity, the Coulomb functions can be replaced by their asymptotic form and amplitude-phase methods can be applied. For the evaluation of these ''tail'' integrals Sil *et al.* [15] study techniques in the complex plane, while Burgess and Sheorey [16] provide an alternative numerical approach. It is obvious that if one should have to calculate an integral of type (3) but only for R to infinity, one could reverse the problem by writing it as Eq. (3) minus the integral from 0 to R.

When a relativistic approach is considered in collision calculations, the integrals involved are not of type (3); the situation is modified in several ways. First of all, there are two components. Secondly, the recursion properties of the Coulomb partial waves linked to the integer nature of angular momenta do not hold. Thirdly, the Coulomb potential whose expansion is the source of the $r^{-\lambda-1}$ term in Eq. (3) is replaced by a photon propagator whose multipole expansion makes Bessel functions appear. A method for evaluating Dirac Coulomb radial integrals is provided, for example, in the paper by Becker *et al.* [17]. The analytical results are much more complicated than in the nonrelativistic case, and recursion relations among them do not seem to be available. Similarly to the study of Sil *et al.* [15], if one considers the tail integrals, i.e., from R to infinity, techniques in the complex plane can be applied effectively whether z_i is equal to z_f or not [18].

E. Illustration

To illustrate some of the theoretical results presented above we consider the electron impact excitation ($z_i=z_f$) and single ionization ($z_f=z_i-1$) of two ions, namely, Mg^+ ($z_i=-1$) and Ar^{7+} ($z_i=-7$). We compare matrix elements calculated with the exact quantal formulation (Sec. II A) and in the WKB approximation (Sec. II B), for the first three multipoles, and for values of angular momenta 0–5 and 15. The Sommerfeld parameters η_i and η_f which enter in all the formulas, have been chosen in the range of the physical situations considered in Sec. III where we shall study the cross section for the electron impact ionization of such ions at moderate energy. The incident energy is fixed at three times the ionization potential (IP) of the target ground state calculated in the frozen-core Hartree-Fock approximation. In atomic units, IP is equal to 0.540 58 and 5.252 24 for Mg^+ and Ar^{7+}, respectively. The corresponding Sommerfeld parameters are ($\eta_i=-0.555\,26$; $z_i=-1$), ($\eta_i=-1.246\,95$; $z_i=-7$) and ($\eta_f=-0.746\,43$; $z_f=-1$), ($\eta_f=-1.492\,86$; $z_f=-2$), ($\eta_f=-1.540\,73$; $z_f=-7$), ($\eta_f=-1.760\,84$; $z_f=-8$).

TABLE I. Comparison between WKB approximation and quantal values of the radial monopole matrix elements $\mathcal{M}_{l,l}^{-1}$ for $z_i=-1(\eta_i=-0.555\,26)$ and $z_f=-1(\eta_f=-0.746\,43)$ or $z_f=-2(\eta_f=-1.492\,86)$.

l	Quantal	WKB
	$z_i=-1;\ z_f=-1$	
0	4.222[−1]	4.819[−1]
1	2.562[−1]	2.710[−1]
2	1.622[−1]	1.675[−1]
3	1.066[−1]	1.089[−1]
4	7.176[−2]	7.287[−2]
5	4.912[−2]	4.968[−2]
15	1.602[−3]	1.590[−3]
	$z_i=-1;\ z_f=-2$	
0	5.351[−1]	5.492[−1]
1	4.530[−1]	4.714[−1]
2	3.407[−1]	3.488[−1]
3	2.467[−1]	2.491[−1]
4	1.766[−1]	1.766[−1]
5	1.261[−1]	1.252[−1]
15	4.726[−3]	4.554[−3]

The quantal and WKB monopole radial matrix elements have been computed by using formulas (4) and (29), respectively. The results are given for Mg^+ in Table I and for Ar^{7+} in Table II.

The quantal dipole radial matrix elements $\mathcal{M}_{0,1}^{-2}$ and $\mathcal{M}_{1,0}^{-2}$ are evaluated through Eq. (6). The recursion formula (21) is then used to generate all the successive dipole terms $\mathcal{M}_{l,l+1}^{-2}$ and $\mathcal{M}_{l+1,l}^{-2}$ with the use of Eq. (4) to calculate the monopole terms $\mathcal{M}_{l,l}^{-1}$. The results are presented in Table III and Table IV for the two ions, respectively. It is important to point out that the use of relation (21) is essential for the evaluation of dipole terms having large values of angular momentum. Indeed, when calculating the second hypergeometric function

TABLE II. Same as Table I but for $z_i=-7(\eta_i=-1.246\,95)$ and $z_f=-7(\eta_f=-1.540\,73)$ or $z_f=-8(\eta_f=-1.760\,84)$.

l	Quantal	WKB
	$z_i=-7;\ z_f=-7$	
0	3.889[−2]	4.011[−2]
1	3.056[−2]	3.142[−2]
2	2.274[−2]	2.321[−2]
3	1.691[−2]	1.717[−2]
4	1.267[−2]	1.282[−2]
5	9.582[−3]	9.671[−3]
15	7.599[−4]	7.595[−4]
	$z_i=-7;\ z_f=-8$	
0	4.537[−2]	4.658[−2]
1	3.725[−2]	3.821[−2]
2	2.869[−2]	2.925[−2]
3	2.182[−2]	2.213[−2]
4	1.661[−2]	1.679[−2]
5	1.269[−2]	1.280[−2]
15	1.046[−3]	1.043[−3]

TABLE III. Comparison between WKB approximation and quantal values of the radial dipole matrix elements $\mathcal{M}_{l,l+1}^{-2}$ and $\mathcal{M}_{l+1,l}^{-2}$ for $z_i=-1(\eta_i=-0.555\,26)$ and $z_f=-1(\eta_f=-0.746\,43)$ or $z_f=-2(\eta_f=-1.492\,86)$.

	$\mathcal{M}_{l,l+1}^{-2}$		$\mathcal{M}_{l+1,l}^{-2}$	
l	Quantal	WKB	Quantal	WKB
	$z_i=-1;\ z_f=-1$			
0	1.779[−1]	1.803[−1]	4.413[−1]	4.386[−1]
1	6.324[−2]	6.421[−2]	2.470[−1]	2.443[−1]
2	2.871[−2]	2.906[−2]	1.499[−1]	1.482[−1]
3	1.478[−2]	1.491[−2]	9.600[−2]	9.482[−2]
4	8.196[−3]	8.253[−3]	6.350[−2]	6.267[−2]
5	4.774[−3]	4.797[−3]	4.291[−2]	4.232[−2]
15	6.311[−5]	6.242[−5]	1.335[−3]	1.304[−3]
	$z_i=-1;\ z_f=-2$			
0	4.086[−1]	4.068[−1]	1.091[−1]	1.123[−1]
1	1.536[−1]	1.539[−1]	1.581[−1]	1.621[−1]
2	7.292[−2]	7.262[−2]	1.411[−1]	1.412[−1]
3	3.881[−2]	3.842[−2]	1.117[−1]	1.101[−1]
4	2.207[−2]	2.175[−2]	8.462[−2]	8.268[−2]
5	1.312[−2]	1.288[−2]	6.293[−2]	6.111[−2]
15	1.886[−4]	1.813[−4]	2.780[−3]	2.633[−3]

F_2 in Eq. (6) convergence is, in most cases, rather slow for large angular momenta. It may also happen that convergence cannot be reached at all as was observed in some of the examples presented here.

The quantal quadrupole radial matrix elements $\mathcal{M}_{l,l+2}^{-3}$ and $\mathcal{M}_{l+2,l}^{-3}$ are directly evaluated through Eq. (6) while the elements $\mathcal{M}_{l,l}^{-3}$ have been computed from dipole matrix elements with formula (25). The results are presented in Table V and Table VI.

In the preceding tables, the dipole and quadrupole WKB radial matrix elements have been obtained by numerical integration of the integral form (28). The accuracy of our integration method was checked for the dipole case by comparing the result for $z_i=z_f$ with that obtained from the analytical form of $\mathcal{I}^{1\pm1}(\epsilon,\xi'=\xi,\ \alpha=0)$ in terms of Hankel functions [see Eq. (II.E.57) in [1]].

In all cases, the values of the WKB radial matrix elements are very close to the quantal ones. The best agreement is achieved with the dipole matrix elements and more generally for Ar^{7+}. This latter result is a consequence of larger values of the Sommerfeld parameters compared to the case of Mg^+.

III. PHYSICAL APPLICATION: COULOMB PROJECTED BORN APPROXIMATION APPLIED TO IONIZATION PROCESSES

To illustrate some of the theoretical results described above, we consider here a physical problem in which matrix elements (3) with $z_i\neq z_f$ appear naturally. Indeed, for the electron impact ionization of a target charged Z, $z_i=-Z$ while $z_f=-Z-1$. Consider the case of ionization of a valence electron in the s ground state, labeled a, to a continuum state, labeled b, of the ejected electron.

TABLE IV. Same as Table III but for $z_i=-7(\eta_i=-1.246\,95)$ and $z_f=-7(\eta_f=-1.540\,73)$ or $z_f=-8(\eta_f=-1.760\,84)$.

l	$\mathcal{M}^{-2}_{l,l+1}$ Quantal	$\mathcal{M}^{-2}_{l,l+1}$ WKB	$\mathcal{M}^{-2}_{l+1,l}$ Quantal	$\mathcal{M}^{-2}_{l+1,l}$ WKB
		$z_i=-7;\ z_f=-7$		
0	5.025[−2]	5.007[−2]	9.385[−2]	9.390[−2]
1	2.483[−2]	2.493[−2]	7.175[−2]	7.163[−2]
2	1.337[−2]	1.344[−2]	5.191[−2]	5.172[−2]
3	7.800[−3]	7.842[−3]	3.772[−2]	3.755[−2]
4	4.819[−3]	4.843[−3]	2.778[−2]	2.763[−2]
5	3.102[−3]	3.115[−3]	2.071[−2]	2.059[−2]
15	1.003[−4]	1.001[−4]	1.549[−3]	1.534[−3]
		$z_i=-7;\ z_f=-8$		
0	6.741[−2]	6.684[−2]	6.377[−2]	6.385[−2]
1	3.324[−2]	3.329[−2]	5.965[−2]	5.977[−2]
2	1.796[−2]	1.803[−2]	4.815[−2]	4.807[−2]
3	1.052[−2]	1.056[−2]	3.739[−2]	3.725[−2]
4	6.525[−3]	6.547[−3]	2.879[−2]	2.863[−2]
5	4.216[−3]	4.226[−3]	2.216[−2]	2.201[−2]
15	1.387[−4]	1.382[−4]	1.870[−3]	1.848[−3]

A. Quantal formulation

In the first-order perturbation theory the triple differential cross section is expressed as

$$\frac{d^3\sigma}{d\Omega_f d\Omega_e dE_e}=\frac{1}{(2\pi)^5}\frac{k_e k_f}{k_i}|T_{if}|^2, \tag{38}$$

with T_{if} given in the Coulomb projected Born approximation [10]

$$T_{if}=\int \mathcal{F}^{-}_{\boldsymbol{k}_f}{}^{*}(\boldsymbol{R})V_T(ab;\boldsymbol{R})\mathcal{F}^{+}_{\boldsymbol{k}_i}(\boldsymbol{R})d\boldsymbol{R}, \tag{39}$$

$$V_T(ab;\boldsymbol{R})=\int \mathcal{F}^{-}_{\boldsymbol{k}_e}{}^{*}(\boldsymbol{r})\left(\frac{1}{|\boldsymbol{r}-\boldsymbol{R}|}-\frac{1}{R}\right)\varphi_a(\boldsymbol{r})d\boldsymbol{r}, \tag{40}$$

where the coordinates $\boldsymbol{R}$ and $\boldsymbol{r}$ correspond to the scattering and the valence electron, respectively. The initial, final, and ejected electrons are described by Coulomb wave functions with momenta k_i, k_f, and k_e, respectively. Considering the closed shell as a spectator, the target ground state may be described by the valence electron wave function φ_a calculated in the frozen-core Hartree-Fock approximation

$$\varphi_a(\boldsymbol{r})=R_{n_a s}(r)Y_{00}(\hat{r}). \tag{41}$$

TABLE V. Comparison between WKB approximation and quantal values of the radial quadrupole matrix elements $\mathcal{M}^{-3}_{l,l+2}$, $\mathcal{M}^{-3}_{l+1,l+1}$ and $\mathcal{M}^{-3}_{l+2,l}$ for $z_i=-1(\eta_i=-0.555\,26)$ and $z_f=-1(\eta_f=-0.746\,43)$ or $z_f=-2(\eta_f=-1.492\,86)$.

l	$\mathcal{M}^{-3}_{l,l+2}$ Quantal	$\mathcal{M}^{-3}_{l,l+2}$ WKB	$\mathcal{M}^{-3}_{l+1,l+1}$ Quantal	$\mathcal{M}^{-3}_{l+1,l+1}$ WKB	$\mathcal{M}^{-3}_{l+2,l}$ Quantal	$\mathcal{M}^{-3}_{l+2,l}$ WKB
			$z_i=-1;\ z_f=-1$			
0	4.533[−2]	4.245[−2]	4.359[−1]	3.835[−1]	1.337[−1]	1.272[−1]
1	1.149[−2]	1.124[−2]	1.014[−1]	9.602[−2]	7.322[−2]	6.984[−2]
2	4.062[−3]	4.033[−3]	3.840[−2]	3.707[−2]	4.373[−2]	4.202[−2]
3	1.715[−3]	1.711[−3]	1.782[−2]	1.733[−2]	2.766[−2]	2.670[−2]
4	8.069[−4]	8.067[−4]	9.231[−3]	9.010[−3]	1.813[−2]	1.754[−2]
5	4.085[−4]	4.085[−4]	5.124[−3]	5.010[−3]	1.217[−2]	1.178[−2]
15	2.348[−6]	2.331[−6]	5.715[−5]	5.568[−5]	3.678[−4]	3.545[−4]
			$z_i=-1;\ z_f=-2$			
0	1.222[−1]	1.103[−1]	5.849[−1]	4.967[−1]	3.830[−3]	9.996[−3]
1	3.130[−2]	2.993[−2]	1.435[−1]	1.316[−1]	2.251[−2]	2.527[−2]
2	1.122[−2]	1.089[−2]	5.808[−2]	5.434[−2]	2.440[−1]	2.502[−2]
3	4.801[−3]	4.677[−3]	2.858[−2]	2.695[−2]	2.102[−2]	2.083[−2]
4	2.286[−3]	2.286[−3]	1.556[−2]	1.473[−2]	1.673[−2]	1.630[−2]
5	1.169[−3]	1.138[−3]	9.009[−3]	8.537[−3]	1.285[−2]	1.240[−2]
15	7.099[−6]	6.821[−6]	1.242[−4]	1.169[−4]	6.343[−3]	5.935[−3]

TABLE VI. Same as Table V but for $z_i=-7$ ($\eta_i=-1.246\,95$) and $z_f=-7$ ($\eta_f=-1.540\,73$) or $z_f=-8$ ($\eta_f=-1.760\,84$).

l	$\mathcal{M}^{-3}_{l,l+2}$ Quantal	$\mathcal{M}^{-3}_{l,l+2}$ WKB	$\mathcal{M}^{-3}_{l+1,l+1}$ Quantal	$\mathcal{M}^{-3}_{l+1,l+1}$ WKB	$\mathcal{M}^{-3}_{l+2,l}$ Quantal	$\mathcal{M}^{-3}_{l+2,l}$ WKB
			$z_i=-7;\ z_f=-7$			
0	4.010[−2]	3.920[−2]	7.721[−1]	6.858[−1]	5.250[−2]	5.391[−2]
1	1.468[−2]	1.440[−2]	1.679[−1]	1.605[−1]	4.541[−2]	4.501[−2]
2	6.240[−3]	6.177[−3]	6.362[−2]	6.196[−2]	3.414[−2]	3.361[−2]
3	3.004[−3]	2.989[−3]	3.053[−2]	2.996[−2]	2.517[−2]	2.475[−2]
4	1.580[−3]	1.576[−3]	1.664[−2]	1.639[−2]	1.864[−2]	1.833[−2]
5	8.855[−4]	8.846[−4]	9.822[−3]	9.693[−3]	1.392[−2]	1.369[−2]
15	1.255[−5]	1.253[−5]	2.362[−4]	2.335[−4]	1.030[−3]	1.013[−3]
			$z_i=-7;\ z_f=-8$			
0	5.585[−2]	5.387[−2]	8.269[−1]	7.335[−1]	2.197[−2]	2.380[−2]
1	2.028[−2]	1.978[−2]	1.822[−1]	1.738[−1]	2.886[−2]	2.933[−2]
2	8.597[−3]	8.482[−3]	7.019[−2]	6.821[−2]	2.598[−2]	2.590[−2]
3	4.136[−3]	4.105[−3]	3.421[−2]	3.349[−2]	2.122[−2]	2.100[−2]
4	2.175[−3]	2.165[−3]	1.892[−2]	1.858[−2]	1.680[−2]	1.658[−2]
5	1.220[−3]	1.216[−3]	1.130[−2]	1.112[−2]	1.315[−2]	1.296[−2]
15	1.744[−5]	1.736[−5]	2.904[−4]	2.863[−4]	1.160[−3]	1.138[−3]

Using the partial wave expansion (1) with $\eta=\eta_e=z_e/k_e=(-Z-1)/k_e$, $\boldsymbol{k}=\boldsymbol{k}_e$ for the Coulomb wave function $\mathcal{F}^{-}_{\boldsymbol{k}_e}{}^{*}(\boldsymbol{r})$, one may write a partial wave expansion for the transition potential

$$V_T(ab;\boldsymbol{R})=\frac{8\pi^{3/2}}{k_e}\sum_{l_e,m_e}(-i)^{l_e}e^{i\delta_{l_e}}\frac{1}{\hat{l}_e}\mathcal{V}_{l_e}(ab;R)\times Y_{l_e,m_e}(\hat{k}_e)Y^{*}_{l_e,m_e}(\hat{R}), \tag{42}$$

with

$$\mathcal{V}_{l_e}(ab;R)=\int_0^\infty rR_{n_as}(r)F_{l_e}(k_e,z_e;r)\times\left(\frac{r^{l_e}_{<}}{r^{l_e+1}_{>}}-\frac{\delta_{l_e0}}{R}\right)dr, \tag{43}$$

where we use the convention $\hat{l}=2l+1$, and $r_<=\min(r,R)$, $r_>=\max(r,R)$. Similarly, one uses Eq. (1) for the Coulomb wave functions $\mathcal{F}^{-}_{\boldsymbol{k}_f}{}^{*}(\boldsymbol{R})$ and $\mathcal{F}^{+}_{\boldsymbol{k}_i}(\boldsymbol{R})$ with $\eta=\eta_f=z_f/k_f$, $\boldsymbol{k}=\boldsymbol{k}_f$ and $\eta=\eta_i=z_i/k_i$, $\boldsymbol{k}=\boldsymbol{k}_i$, respectively. Taking the direction of the initial momentum $\boldsymbol{k}_i$ to be along the z axis, we obtain the simplified expression of the CPB triple, double, and single differential cross sections

$$\frac{d^3\sigma}{d\Omega_f d\Omega_e dE_e}=\frac{32k_f}{k_ik_e}\left|\sum_{l_e,m_e,l_i,l_f}i^{(l_i-l_e-l_f)}e^{i[\delta_{l_i}+\delta_{l_e}+\delta_{l_f}]}\times\mathcal{A}^{l_e}_{l_il_f}\mathcal{R}^{l_e}_{l_il_f}Y_{l_e,m_e}(\hat{k}_e)Y_{l_f,-m_e}(\hat{k}_f)\right|^2, \tag{44}$$

$$\frac{d^2\sigma}{d\Omega_f dE_e}=\frac{32k_f}{k_ik_e}\sum_{l_e,m_e}\left|\sum_{l_i,l_f}i^{(l_i-l_f)}e^{i[\delta_{l_i}+\delta_{l_f}]}\times\mathcal{A}^{l_e}_{l_il_f}\mathcal{R}^{l_e}_{l_il_f}Y_{l_f,-m_e}(\hat{k}_f)\right|^2, \tag{45}$$

$$\frac{d\sigma}{dE_e}=\frac{32k_f}{k_ik_e}\sum_{l_i,l_e,l_f}\frac{\hat{l}_i\hat{l}_f}{\hat{l}_e}\begin{pmatrix}l_i & l_e & l_f\\ 0 & 0 & 0\end{pmatrix}^2[\mathcal{R}^{l_e}_{l_il_f}]^2, \tag{46}$$

where

$$\mathcal{A}^{l_e}_{l_il_f}=\hat{l}_i\hat{l}_e{}^{-1/2}\hat{l}_f{}^{1/2}\begin{pmatrix}l_i & l_e & l_f\\ 0 & 0 & 0\end{pmatrix}\begin{pmatrix}l_i & l_e & l_f\\ 0 & -m_e & m_e\end{pmatrix},$$

$$\mathcal{R}^{l_e}_{l_il_f}=\frac{1}{k_ik_f}\int_0^\infty F_{l_i}(k_i,z_i;R)\mathcal{V}_{l_e}(ab;R)\times F_{l_f}(k_f,z_f;R)dR. \tag{47}$$

It is clear that matrix elements of the type given in Eq. (3) appear in the radial integrals (47) since the radial part $\mathcal{V}_\lambda$ of the transition potential V_T behaves asymptotically as $1/R^{\lambda+1}$ ($\lambda>0$). Before describing the results obtained in a practical example, we would like to show how the singly and doubly differential cross sections may be evaluated in the semiclassical approximation, since the integrals involved have a close connection with those presented in Sec. II B.

B. WKB and semiclassical formulations

In the semiclassical picture [1], the projectile is assumed to follow a classical Coulomb trajectory and the ionization of the target is described in the framework of the first-order time dependent perturbation theory. This perturbation is assumed not to affect the projectile trajectory. The double differential ionization cross section is written as

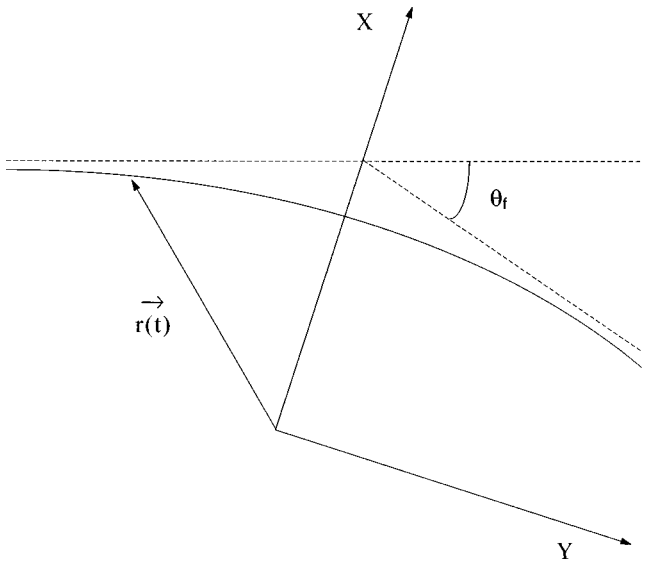

FIG. 1. Classical picture of the electron orbit in the Coulomb field of the positive ion. The position of the electron and the deflection angle are denoted by $\mathbf{r}(t)$ and θ_f, respectively.

$$\frac{d^2\sigma}{d\Omega_f dE_e} = P_{ab}\left[\frac{d\sigma}{d\Omega_f}\right]_R \frac{k_e}{(2\pi)^3}, \tag{48}$$

with the Rutherford cross section given by

$$\left[\frac{d\sigma}{d\Omega_f}\right]_R = \frac{1}{4}\tilde{a}^2 \frac{1}{\sin^4(\theta_f/2)} \tag{49}$$

and where $\tilde{a}$ is the characteristic length of the scattering problem. The probability of ionization from the ground state a to the continuum state b is given by

$$P_{ab} = \int |b_{ab}|^2 d\hat{k}_e, \tag{50}$$

with

$$b_{ab} = \frac{1}{i}\int_{-\infty}^{+\infty} e^{i\Delta E t} V_T(ab;\boldsymbol{R}(t))dt. \tag{51}$$

In the preceding expression, the time integration is performed along an average Rutherford trajectory (see Fig. 1). After some algebraic manipulations one finally obtains

$$\frac{d^2\sigma}{d\Omega_f dE_e} = \frac{8\tilde{a}^2}{k_e k_i^2}\left\{\sum_{l_e,m_e} \frac{1}{(2l_e+1)^2} \times \left| Y_{l_e,m_e}\left(\frac{\pi}{2},0\right)\mathcal{J}^{l_e m_e}(\epsilon_c,\xi',\alpha,\tilde{a})\right|^2\right\}\left[\frac{d\sigma}{d\Omega_f}\right]_R, \tag{52}$$

$$\frac{d\sigma}{dE_e} = \int \frac{d^2\sigma}{d\Omega_f dE_e} d\Omega_f, \tag{53}$$

with

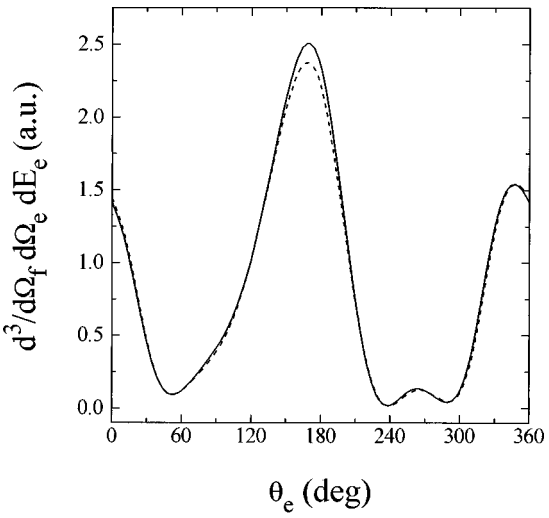

FIG. 2. Calculated triple differential cross section in atomic units for the $(e\text{-}2e)$ ionization of the alkali-metal-like ion Mg^+ in coplanar geometry. The incident energy is equal to four times the ionization energy calculated in the frozen-core Hartree-Fock approximation and the energy of the slow ejected electron is 5 eV. The scattering angle θ_f is fixed at 4°. The quantal (CPB) and WKB predictions are represented by the solid line and by the dashed line, respectively.

$$\mathcal{J}^{l_e m_e}(\epsilon_c,\xi',\alpha,\tilde{a}) = \int_{-\infty}^{+\infty} e^{i\xi'[\epsilon_c \sinh(x)+x+(\alpha/\xi')x]} \times \mathcal{V}_{l_e}\{\tilde{a}[\epsilon_c\cosh(x)+1]\} \times \frac{[\cosh(x)+\epsilon_c+i\sqrt{\epsilon_c^2-1}\sinh(x)]^{m_e}}{[\epsilon_c\cosh(x)+1]^{m_e-1}}dx, \tag{54}$$

where the quantities $\tilde{a}$, ϵ_c are defined by

$$\tilde{a} = \frac{\tilde{\eta}}{\tilde{k}},$$

$$\epsilon_c = \mathrm{sgn}(\tilde{z})/\sin(\theta_f/2). \tag{55}$$

The connection between the semiclassical integrals and the quantal Coulomb integrals is given by the WKB approximation through the following relation between Eq. (54) and the radial integral (47):

$$\mathcal{R}^{l_e}_{l_i l_i+\mu} = \frac{\tilde{a}}{4\tilde{k}^2}\mathcal{J}^{l_e\mu}(\epsilon_c,\xi',\alpha,\tilde{a}). \tag{56}$$

C. Numerical results

In all the numerical results presented in this section, the WKB approximation of the TDCS, DDCS, and SDCS was obtained by employing the WKB formula (56) for the radial matrix elements instead of the quantal one (47).

In Fig. 2 we compare the predictions of the WKB and quantal (CPB) TDCS for the $(e\text{-}2e)$ ionization of the alkali-metal-like ion Mg^+ in coplanar geometry where the scatter-

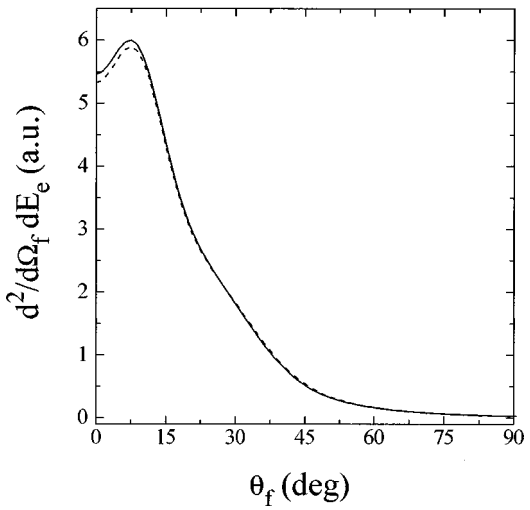

FIG. 3. Calculated double differential cross section in atomic units for the $(e\text{-}2e)$ ionization of the alkali-metal-like ion Mg^+ in coplanar geometry. The incident energy is equal to four times the ionization energy calculated in the frozen-core Hartree-Fock approximation and the energy of the slow ejected electron is 5 eV. The quantal (CPB) and WKB predictions are represented by the solid line and by the dashed line, respectively.

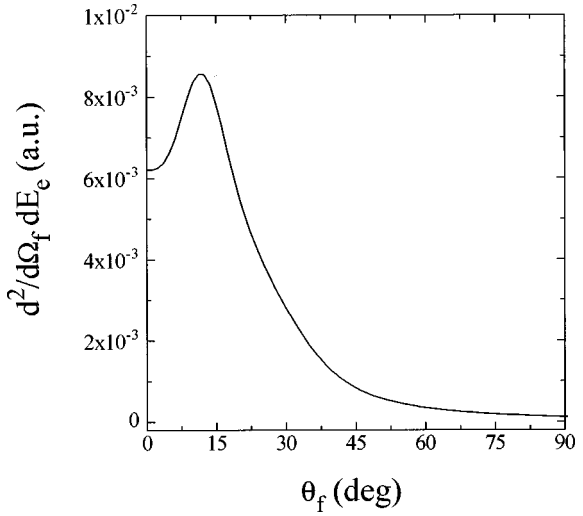

FIG. 4. Quantal (CPB) double differential cross section in atomic units for the $(e\text{-}2e)$ ionization of the alkali-metal-like ion Ar^{7+} in coplanar geometry. The WKB prediction cannot be visually distinguished from the quantal curve. The incident energy is equal to four times the ionization energy calculated in the frozen-core Hartree-Fock approximation and the energy of the slow ejected electron is 5 eV.

ing angle is fixed at 4°. The incident energy is equal to four times the ionization potential, while the slow ejected electron takes 5 eV (0.183 75 atomic units) giving the following Sommerfeld parameters ($\eta_i=-0.480\,87$; $z_i=-1$) and ($\eta_f=-1.179\,33$; $z_f=-2$). The radial matrix elements have been computed as explained in Sec. II E. The agreement is seen to be very good despite the rather low value of the Sommerfeld parameters involved. At the same ratio $X=E_i/\mathrm{IP}$, for alkali-metal-like ions of higher values of the ionic charge the agreement between quantal and WKB predictions becomes so perfect that the curves are almost indistinguishable.

In Fig. 3 we show the DDCS which corresponds to the integration of the preceding TDCS of Fig. 2 over the angular range of the ejected electron, and in Fig. 4 the DDCS for the $(e\text{-}2e)$ ionization of another alkali-metal-like ion, Ar^{7+}, with the same energy ratio X. For this target the Sommerfeld parameters are ($\eta_i=-1.079\,89$; $z_i=-7$) and ($\eta_f=-1.433\,47$; $z_f=-8$). Since the initial state has spherical symmetry (s state), the DDCS does not altogether depend on the azimuthal angle ϕ_f of $\boldsymbol{k}_f$. As for the TDCS, the WKB and quantal predictions are in very good agreement. Note that we have not reproduced the WKB predictions in Fig. 4 since the differences with the quantal ones are not visible on the scale of the figure.

Compared to what is generally observed in the ionization of neutral atoms, the quantal DDCS exhibits a new feature: the angular distribution is no longer peaked at zero degree. This shift of the maximum of the differential cross section was first emphasized by Mitroy [19] in the context of electron impact excitations of positive ions. One can estimate the position of this maximum by using semiclassical arguments. In order to transfer the energy ΔE from the relative motion to the target, the collision time τ_c should be lower than $1/\Delta E$. Here we have $\Delta E=\mathrm{IP}+E_e$, IP being the ionization potential and E_e the energy of the ejected electron. Thus, on an average Coulomb trajectory the collision time may be estimated by

$$\tau_c=\frac{r_{\min}}{k_i}=\frac{\tilde{a}(1+\epsilon_c)}{k_i},$$

which leads to the following estimate of the critical angle θ_{cr} below which there is no transition:

$$\theta_{\mathrm{cr}}=2\arcsin\left(\frac{\xi'}{\xi'+1}\right). \tag{57}$$

Concerning the examples in which we are interested, the above formula gives $\theta_{\mathrm{cr}}\sim 15°$ and $\theta_{\mathrm{cr}}\sim 18°$ for Mg^+ and Ar^{7+}, respectively. As can be seen in Fig. 3 and Fig. 4 these are good estimates of the quantal predictions.

By integration of the DDCS over the scattering angles one obtains the SDCS. The predictions of the quantal, WKB and semiclassical approximation for Mg^+ and for different values of the ratio X are given in Table VII. The semiclassical

TABLE VII. Quantal, WKB, and semiclassical (SC) single differential cross sections in atomic units for the ionization by electron impact of the sodiumlike ion Mg^+ ($z_i=-1$ and $z_f=-2$). The incident energy is equal to X times the ionization energy calculated in the Hartree-Fock approximation. The energy of the ejected electron is fixed at 5 eV.

X	Quantal	WKB	SC
2	8.379	8.330	8.384
3	5.872	5.854	5.866
4	4.578	4.569	4.574
5	3.778	3.773	3.777
6	3.230	3.227	3.230

results have been obtained by using expressions (52) and (53). One immediately notes that the quantal and semiclassical predictions agree within less than 0.1%, the difference between quantal and WKB results being a little less than 0.6% in the worst case.

Furthermore, we have checked that, in a wide range of energy, energy transfer, and ionic charge, the semiclassical single differential cross sections are always practically equal to the quantal predictions. As already shown in [9] this almost perfect agreement between the quantal and semiclassical description is strongly related to the validity of the WKB approximation. This is reminiscent of the equivalence of the semiclassical and Born approximation in the calculation of inelastic cross sections integrated over angles.

ACKNOWLEDGMENTS

One of us (L.U.A.) would like to acknowledge financial support from Trinity Hall, Cambridge. The authors would also like to thank the Centre National Universitaire Sud de Calcul (CNUSC) for providing free computer time.

[1] K. Alder, A. Bohr, T. Huus, B. Mottelson, and A. Winther, Rev. Mod. Phys. **28**, 432 (1956).
[2] A. Burgess, D. G. Hummer, and J. A. Tully, Philos. Trans. R. Soc. London, Ser. A **266**, 225 (1970).
[3] A. Burgess, J. Phys. B **7**, L364 (1974).
[4] L. C. Biedenharn, J. L. McHale, and R. M. Thaler, Phys. Rev. **100**, 376 (1955).
[5] K. W. Ford and J. A. Wheeler, Ann. Phys. (N.Y.) **7**, 259 (1959).
[6] W. F. Egelhoff, Phys. Rev. Lett. **71**, 2883 (1993).
[7] M. Bachmann, Z. Halabuka, and D. Trautmann, J. Phys. B **28**, 631 (1995).
[8] M. Chidichimo and M. Stastna, Phys. Rev. A **53**, 1519 (1996).
[9] P. A. Hervieux and C. Guet, Phys. Rev. A **47**, 2031 (1993).
[10] S. Geltman and M. B. Hidalgo, J. Phys. B **7**, 831 (1974).
[11] C. Dal Cappello, R. El Mkhanter, and P. A. Hervieux, Phys. Rev. A **57**, R693 (1998).
[12] *Handbook of Mathematical Functions*, edited by M. Abramowitz and I. A. Stegun (Dover, New York, 1970).
[13] S. Nakazaki, J. Phys. Soc. Jpn. **45**, 225 (1978).
[14] K. Alder and A. Winther, K. Dan. Vidensk. Selsk. Mat. Fys. Medd. **31**, No. 1 (1956).
[15] N. C. Sil, M. A. Crees, and M. J. Seaton, J. Phys. B **17**, 1 (1984).
[16] A. Burgess and V. B. Sheorey, J. Phys. B **7**, 2403 (1974).
[17] U. Becker, N. Grün, and W. Scheid, J. Phys. B **19**, 1347 (1986).
[18] L. U. Ancarani, S. Keller, H. Ast, C. T. Whelan, H. R. J. Walters, and R. M. Dreizler, J. Phys. B **31**, 609 (1998).
[19] J. Mitroy, Phys. Rev. A **37**, 649 (1988).